Polarized Compartmentalization of Organelles in Growth Cones from Developing Optic Tectum

T. P. O. CHENG and T. S. REESE
Laboratory of Neurobiology, Intramural Program, National Institute of Neurological Communicative Disease and Stroke, at Marine Biological Laboratory, National Institutes of Health, Woods Hole, Massachusetts 02543

ABSTRACT We have used computer-assisted reconstructions of continuous serial sections to study the cytoplasmic organization of growth cones in vivo. Optic tecta from 6.25–6.5-d-old chicken embryos were quick-frozen and then freeze-substituted in acetone-osmium tetroxide or, for comparison, prepared by conventional fixation. Images of eight freeze-substituted and two conventionally fixed growth cones were reconstructed from aligned serial micrographs. After freeze-substitution, numerous lumenless membrane-bound sacs arrayed in multilamellated stacks appear to replace the abundant smooth endoplasmic reticulum found after chemical fixation. Microtubule fascicles progressively diverge from their typical fascicular organization in the initial segment of the growth cone and are absent in the varicosity and the more distal segment. Mitochondria, in contrast, are concentrated in the proximal segment of the varicosity; multilamellated stacks and endosomelike vacuoles are in the distal segment; and coated pits and vesicles are concentrated near the terminal filopodium, which is the most distal and organelle-poor domain of the growth cone. These observations suggest that dilation and fusion of the lumenless, membrane-bound sacs that occurs during chemical fixation give rise to the network of smooth endoplasmic reticulum. The three-dimensional reconstructions show that the cytoplasmic components of growth cones, including the membrane-bound sacs and multilamellated stacks revealed by freeze substitution, are polarized along the axis of these growth cones, which suggests that they have a role in recycling of membrane during elongation of the growth cone.

Growth cones are found at the tips of the growing or regenerating processes of a neuron. They are characterized by a single cone-shaped varicosity with several radiating filopodia or lamellopodia (1, 12, 31, 35). Numerous membrane-bound organelles, in addition to cytoskeletal elements and the cytomatrix, are located in the varicosity. These include smooth endoplasmic reticulum (SER),[1] mitochondria, lysosomes, coated and dense-core vesicles, and subplasmalemmal vesicles (4, 16, 17, 24, 29, 37, 41).

During neuronal development, processes grow out from the cell body of a neuron to reach specific target cells, so growth cones may be responsible not only for recognition of target cells but also for the guidance of the growing neurites (1, 9, 17, 20, 28, 34, 38). Because of the labile nature of the growing neuritic tips, it is not surprising that they are highly polarized structures. The number of integral membrane proteins at the cell body, represented as intramembrane particles, is reported to be greated than that at neurites which, in turn, have more particles than growth cones, so there is a gradient in the concentration of these membrane components from the cell body to the neurite tip (25, 33). Also, the regional distribution of various kinds of surface receptors in a developing neuron varies systematically along its growing axis (26). Although there are these indications of morphological polarity in the plasmalemma, little is known about the differential distribution of intracellular organelles and cytoplasmic structures in a growth cone.

To analyze this fundamental relationship between structure and function in growth cones, we studied growth cones in their natural location in the chick optic tectum. This preparation has been widely used to study formation of specific

[1] *Abbreviation used in this paper:* SER, smooth endoplasmic reticulum.

connections in the vertebrate brain during development (27a). The interactions of the tectal growth cones with the three-dimensional matrix of extracellular substances and other cellular structures in the neuropil were expected to provide a more realistic picture of the native, dynamic shape and organization of developing growth cones. Furthermore, we employed a combination of cryotechniques (quick-freezing and freeze-substitution) in order better to preserve labile membrane structures (27a), and made computer-aided, large scale serial reconstructions in order to create a three-dimensional picture of the distribution of cytoplasmic organelles. We have identified a novel multilamellated membrane organelle and also demonstrated that intracellular organelles distribute differentially and systematically along the longitudinal axis of growth. This polarization of cytoplasmic compartments along the growing axes of the growth cones leads to new conclusions about their specific functions.

MATERIALS AND METHODS

Preparation of Specimens for Cryogenic and Chemical Fixation: Fertile white Leghorn eggs (Spafas Inc., Norwich, CT) were incubated in a forced draft incubator at 37°C. Chicken embryos were selected at different stages of incubation according to the Hamburger and Hamilton series (11) and placed into minimum essential medium with Hanks' salts (Gibco Laboratories Inc., Grand Island, NY) supplemented with 10% fetal bovine serum (Gibco Laboratories Inc.), 0.4% D-glucose, and saturated with oxygen at 37°C (conditions typically used for maintaining dissociated neurons in culture preparations; 4). After the overlying vascular tissues were removed, the optic tecta were dissected out, gently placed onto a planchet with a spatula, and immediately slam-frozen against a copper block cooled with liquid helium (14). The time from removal of the vascular tissue until freezing was typically 2 min. Each specimen was positioned so that it was the rostroventral surface of the tectum that made initial contact with the cold block. Frozen samples were either processed for freeze-substitution or stored in liquid nitrogen for later use.

For freeze-substitution, samples were submerged in liquid nitrogen-filled vials containing 4–5% OsO_4 in 100% acetone. After a 17-h period of freeze-substitution at −78°C, the vials were warmed gradually to −40°C inside a freezer (So-Low Environmental Equipment Co., Inc., Cincinnati, OH), rinsed three times with precooled acetone, fixed in another acetone mixture containing 5% acrolein and 0.5% tannic acid for 5 h, and then warmed to −20°C (3). While then warmed from −20 to 0°C, samples were rinsed several times with precooled acetone to remove any residual fixative. After being transferred to absolute methanol, they were stained with 20% uranyl acetate in 100% methanol at 0°C overnight. Finally, they were rinsed with 100% methanol, warmed to room temperature, and processed by routine epoxy embedding techniques for electron microscopy.

For conventional chemical fixation, embryos at comparable stages of development were perfused through the heart with 0.2 M sodium cacodylate buffer, pH 7.2, containing 2% paraformaldehyde, 2% glutaraldehyde, 0.5% acrolein, and 0.5% tannic acid. After 15 min of perfusion, the optic tecta were removed and left in fixative overnight at 0°C. They were then rinsed with 0.2 M cacodylate buffer. A narrow strip of tectal tissue (~2 mm wide) was dissected out along the rostrocaudal axis of each tectum. The strip was cross-sectioned into five pieces, and the orientation of each of the five pieces was marked by cutting off a corner. The resulting pieces were then postfixed individually for 1 h with 2% OsO_4 in 0.2 M cacodylate buffer, pH 7.2, at 0°C. After osmication, the samples were rinsed in acetate buffer, stained in 2% aqueous uranyl acetate for 1 h at room temperature, and flat-embedded by the same technique as that used for the freeze-substituted tecta. The ordering and orientation of the tectal pieces were maintained throughout the preparation so the orientation of thin-sectioned growth cones could be estimated; knowledge of their appearance when cut in various planes helped us eventually to identify the axis of growth cones seen in the quick-frozen specimens, where the orientation of the tectal pieces was lost.

Computer-aided Reconstruction of Serial Sections: Typically, a ribbon of ~250 sections was cut at 90-nm thickness with a diamond knife on a Sorvall Porter-Blum MT2-B (E. I. DuPont de Nemours & Co., Inc., Sorvall Instruments Div., Newtown, CT) or Reichert ultramicrotome (Reichert AG, Vienna). The ribbon was subdivided into 10 sequential short ribbons, each of which was collected on a Formvar-coated slot grid. After heavy-metal grid staining, the serial sections were air-dried overnight and then examined in a JEOL 200-CX electron microscope at 120 kV.

During printing of a series, each structure of interest was aligned in best-fit registration with respect to the previous section. The top and the left-hand sides of an 8 × 10 sheet of printing paper were used as lines of reference which remained unchanged throughout the printing of a series. Typically, the first micrograph of a series was used as a template to align the projected optical image of the subsequent negative. After alignment, the projected image was printed, and the resulting micrograph was, in turn, used to align the next negative of the series. This procedure of finding the best match between the projected image and the previously printed image was repeated until a series had been completed. Each micrograph (final magnification, 32,500) of a series realigned using the edges of the print for reference. The outlines of each structure of interest were traced and then digitized with a Zeiss Videoplan IV Graphic System (Carl Zeiss, Inc., Thornwood, NY). Because of a limitation in computer memory, only every second or third section in a series could be processed. After a series had been traced, the digital data were manipulated so as to rotate reconstructed images of growth cones to a desirable angle of perspective and to remove hidden lines. The final data were then plotted and the resulting reconstructions were projected on a video monitor.

RESULTS

Initial examination of chemically fixed and of quick-frozen specimens indicated that tecta from embryos at 6.25–6.5 d of incubation were most suitable for the present studies. At this early stage of development, growth cones, as identified by their irregular outlines and cone-shaped varicosities, were abundant in the superficial region of the tectal plate. They were divided into fascicles laterally and superficially by the radial glial fibers, which were distinguished by their darker staining cytoplasm, in part due to their high content of ribosome-like particles.

Growth cones in the quick-frozen and freeze-substituted specimens contained, in addition to cytoskeletal elements, numerous membrane-bound organelles; these organelles included endosome-like vacuoles (Fig. 1), coated pits and vesicles (Fig. 2), and stacks of lumenless membrane-bound organelles, a structure not found in chemically fixed growth cones (Figs. 1 and 3). No moundlike structures or clusters of subplasmalemmal vesicles (24) were found in the quick-frozen growth cones though they were common in the chemically fixed ones (Fig. 4). Other distinctive features of the frozen growth cones were the paucity of SER (Fig. 2) and the absence of myelin figures. Myelin figures were typically located near the mounds (Fig. 4), less frequently near the SER network in the fixed growth cones (Fig. 5 and Fig. 5, inset).

Cytoplasmic Compartmentation and Spatial Polarization

Reconstruction of 10 series of sections through growth cones (8 freeze-substituted and 2 chemically fixed) at 6.25–6.5 d of incubation revealed spatial differences in the distribution of intracellular organelles along the growing axis of the growth cone, suggesting a polarized differential distribution of organelles along the longitudinal axis of the growing neuronal tips.

Enlargement of the neurite marked the initial segment, or transition zone, of the growth cone. The continuation of the initial segment became the varicosity which, in turn, gradually tapered to form the terminal filopodium. Typically, each growth cone had one long (>6 μm long, n = 10) terminal filopodium and several short (<2 μm long, n = 52) subterminal filopodia. The microtubule fascicles, which were prominant and well organized in the neuritic shaft (Figs. 6 and 7), were less distinct in the transition zone (Fig. 8, section 6), and

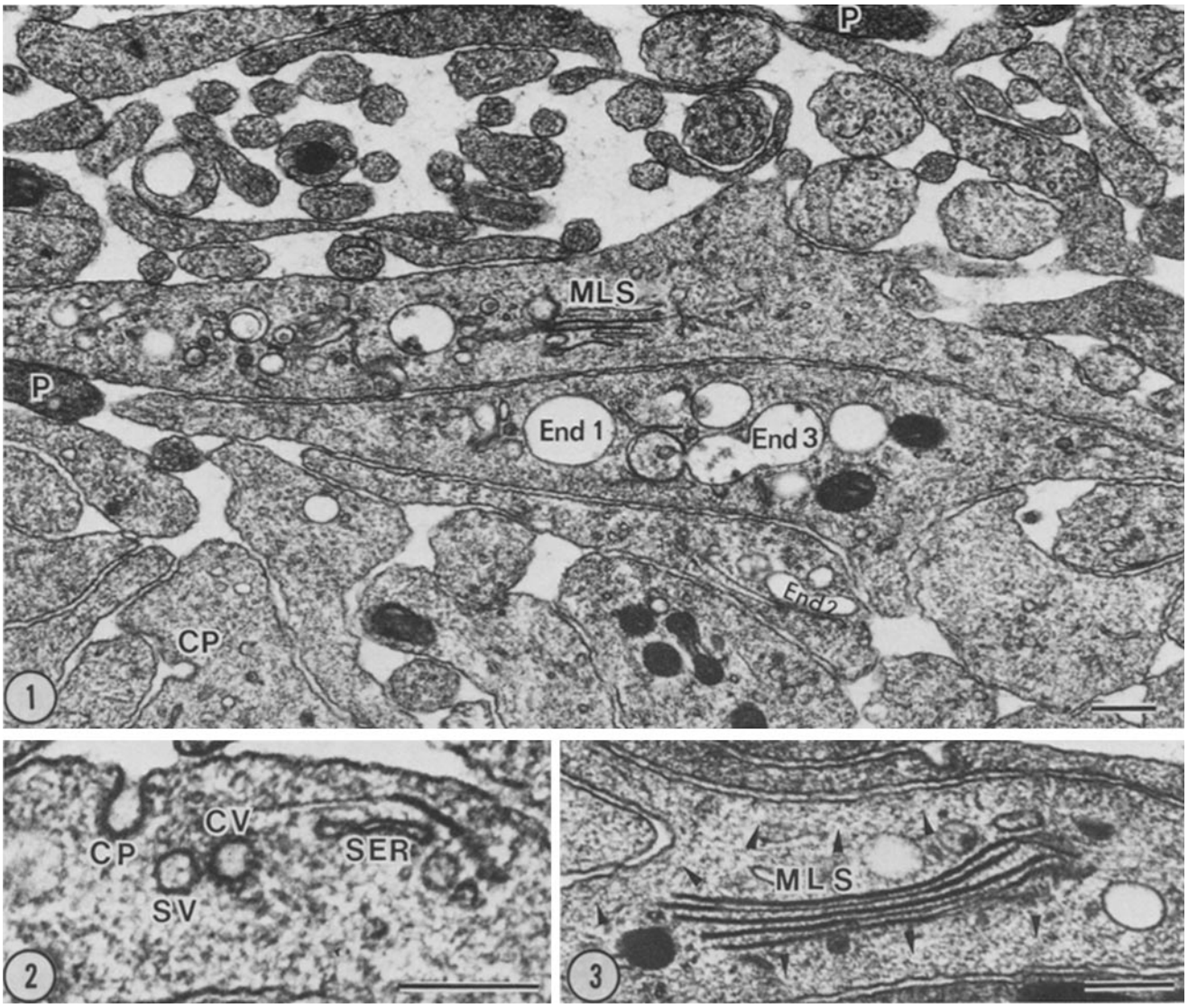

FIGURES 1–3 Quick-frozen growth cones from chick optic tectum (Fig. 1) showing endosome-like vacuoles (*End 1–3*). Most endosomes are spherical (*End 1*), some are flattened (*End 2*), and others appear to be fusing (*End 3*). Coated pits (*CP*), coated vesicles (*CV*), and smooth or uncoated vesicles (*SV*) are common in the filopodia and the varicosity of the growth cone (Fig. 2), whereas sacs of smooth endoplasmic reticulum (*SER*) are rare. Multilamellated stacks (*MLS*) are characteristic of the quick-frozen growth cones (Figs. 1 and 3). Organelles are typically excluded from the subplasmalemmal cortical areas (indicated by arrowheads in Fig. 3). *P*, glial process. Bar, 0.25 μm.

essentially absent from the varicosity and the more distal regions of the growth cone (Fig. 8, sections 25, 90, and 102). The number of microtubules in the growth cone also decreased progressively from proximal to distal, and eventually only a couple of isolated microtubules extended to the end of the terminal filopodium (Fig. 8, sections 116 and 128). Although microtubule bundles occasionally appeared to diverge from the main fascicle into the vicinity of subterminal filopodia, there were no examples of the isolated bundles that would be expected if microtubule bundles looped back (40).

In contrast, concentrations of the various membrane-bound organelles (mitochondria, endosome-like vacuoles, stacks of lumenless membrane-bound sacs, coated pits, and coated vesicles) appeared in different successive regions of the varicosity. Groups of endosome-like vacuoles (diameter >150 nm, $n = 130$) and uncoated vesicles (diameter <100 nm, $n = 85$) were located very close to and among concentrations of the lumenless membrane-bound sacs and the multilamellated stacks, which suggests that the endosome-like vacuolar membrane system may be functionally related to the lumenless membrane-bound sacs in the multilamellated stacks. Coated pits and coated vesicles were concentrated distal to the concentrations of the vacuoles and the lumenless membrane-bound sacs, much less concentrated at the initial regions of the subterminal filopodia, and found only occasionally in the neurite and the more proximal regions of the growth cones. Membrane-limited organelles were rare in the terminal filopodium. This organelle-poor domain of the growth cone had a cytoplasmic ground substance resembling that in the subplasmalemmal cortical region of the growth cone proper. At higher resolution, this ground substance appeared to be a meshwork of fine filaments of various diameters. It appeared also to be more concentrated in the terminal filopodium than in the other regions of the growth cone, based on the staining intensity with uranium and lead.

Typical spatial distributions of microtubule bundles and

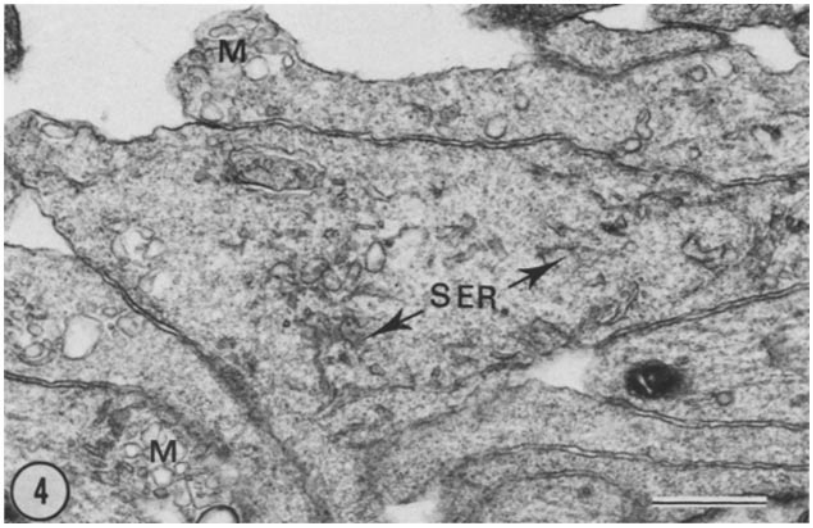

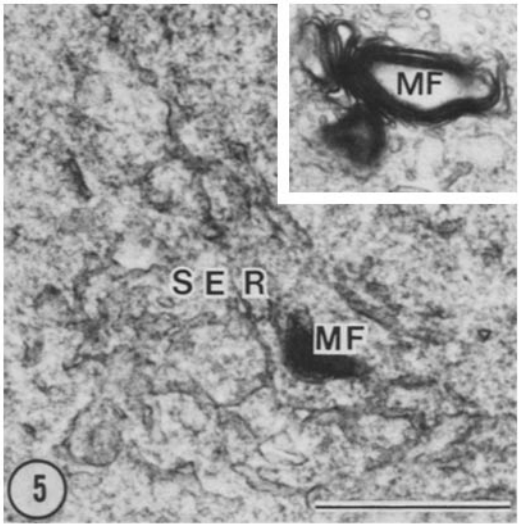

FIGURES 4 and 5 Chemically fixed growth cones from chick optic tectum. Numerous moundlike (*M*) structures occur after chemical fixation (Fig. 4); these are typically located at the tips or bases of filopodial processes. The other predominant structure in the fixed growth cones is an anastomosing SER. Myelin figures (*MF*, Fig. 5 and inset) are common near mounds (*M*) but are less frequent near the SER. Bar, 0.5 μm.

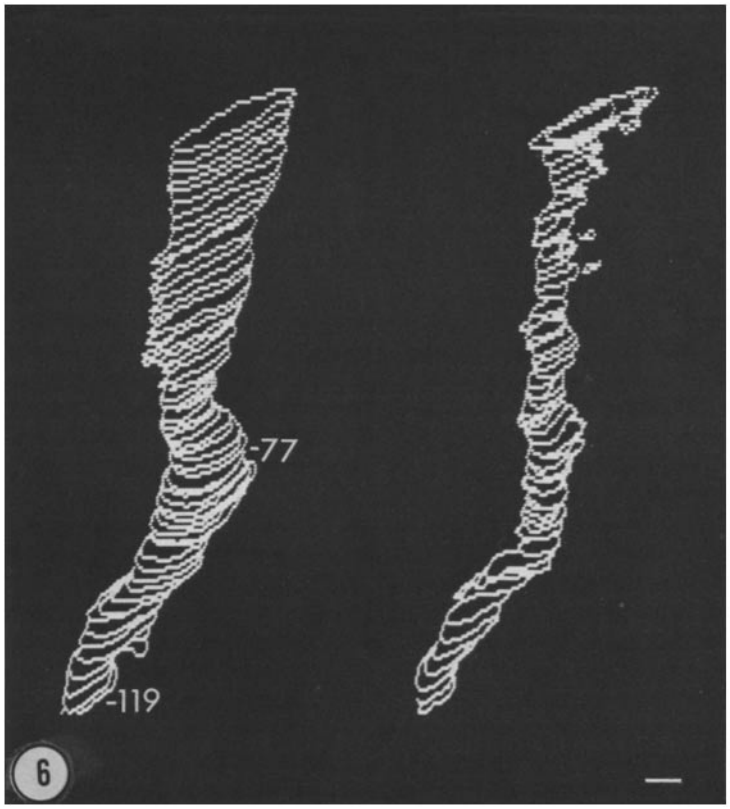

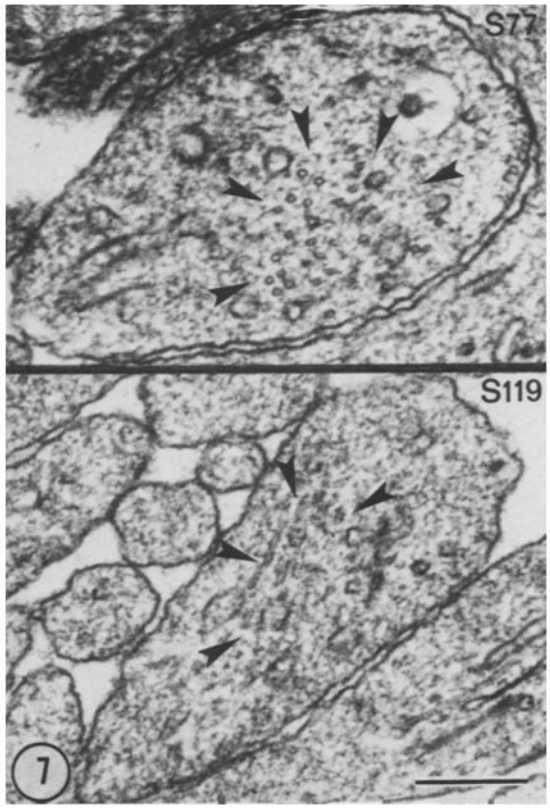

FIGURES 6 and 7 Serial reconstruction of a neurite (Fig. 6, *left*) and the distribution of its microtubule bundle (*right*) from a series of 60 alternate sections, exemplified by sections 77 (*S77*, Fig. 7, *top*) and 119 (*S119*, *bottom*). Typically, microtubules form a single fascicle in the neuritic shaft (outlined by arrowheads in Fig. 7, *S77*), which diverges into individual small bundles (*S119*) at the transition zone of the growth cone. Bar, 0.25 μm.

the various membrane-bound organelles along the longitudinal axis of growth cones are shown in the serial reconstructions (Fig. 9). Five structural domains are delineated along the longitudinal axis of the growth cones on the basis of the spatial distributions of the intracellular organelles: the terminal neurite, the transition zone, the proximal and the distal segments of the varicosity, and the terminal filopodium.

The serial reconstructions were used to measure the density of coated pits, microtubules, mitochondria, coated vesicles, endosome-like vacuoles, and multilamellated stacks of lumenless membrane-bound sacs (membrane disks) in the structural domains along the axis of the growth cone. The polarization of the cytoplasmic compartments, as defined by the distribution of intracellular organelles in the growth cones, was evi-

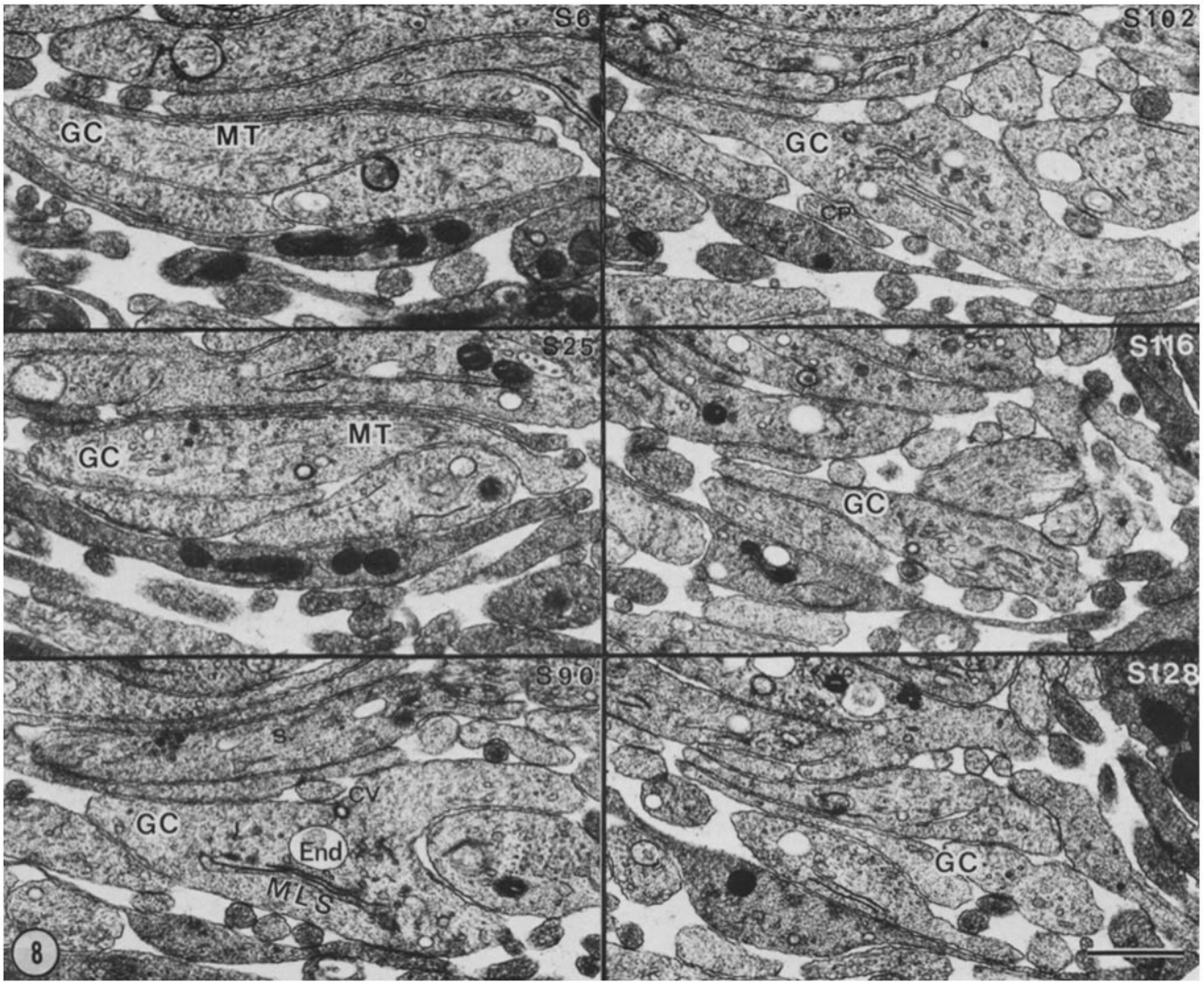

FIGURE 8 Selected serial sections from a quick-frozen growth cone (*GC*). These serial electron micrographs of sections (*S*) 6, 25, 90, 102, 116, and 128 illustrate definitive features of morphological organization along the axis of growth (see Fig. 9 for location of these sections in growth cone). The complete reconstruction of this growth cone is illustrated in Fig. 9. At the transition zone (*S6*), microtubule bundles (*MT*) diverge into individual small fasicles. They become more disorganized and divergent by section 25 (beginning of a varicosity), and are absent from sections 90, 102, 116 (varicosity), and 128 (terminal filopodium). Meanwhile, other organelles (multilamellated stack, *MLS*; endosomelike vacuole, *END*; coated pits, *CP*; coated vesicle, *CV*) appear in sections 90, 102, and 116 and, in turn, disappear in section 128, giving way to the terminal filopodium, which branches off to the right. Bar, 0.5 μm.

dent when these measurements were pooled (Fig. 10). These measurements confirmed the observed differences in the distribution of various organelles listed above.

DISCUSSION

Application of quick-freezing and freeze-substitution to prepare growth cones in intact optic tectum has enabled us to identify a novel intracellular, multilamellated organelle in the body of the growth cone. Some of the multilamellated stacks of lumenless membrane-bound disks appear to be converted to myelin figures during conventional fixation, whereas others dilate and fuse to form the anastomosing SER. Large quantities of SER network have also been observed in growth cones that have been fixed chemically (4, 5, 40). In contrast, SER is rare in the quick-frozen and freeze-substituted growth cones. Glutaraldehyde fixation, even in conjunction with postosmication, apparently can deform existing membrane organelles and generate new structures such as the mounds or subplasmalemmal clusters of 70–300 nm vesicles (see reference 29).

The shape of the freeze-substituted growth cones is significantly different from those usually seen in cultures of dissociated neurons. The varicosity of the typical freeze-substituted growth cone is bulbous with one long terminal filopodium and several short subterminal filopodia, in contrast to those in culture which have numerous radiating filopodia or lamellopodia (2, 4, 12, 18, 21, 24, 25, 31, 35, 40). The differences between the shapes of growth cones from intact optic tectum prepared by freeze-substitution and those of growth cones in culture prepared by chemical fixation could not have resulted from the different preparative techniques because these differences are not found between tectal growth cones that have been freeze-substituted or chemically fixed. Thus, differences in shape and numbers of filopodia must reflect differences

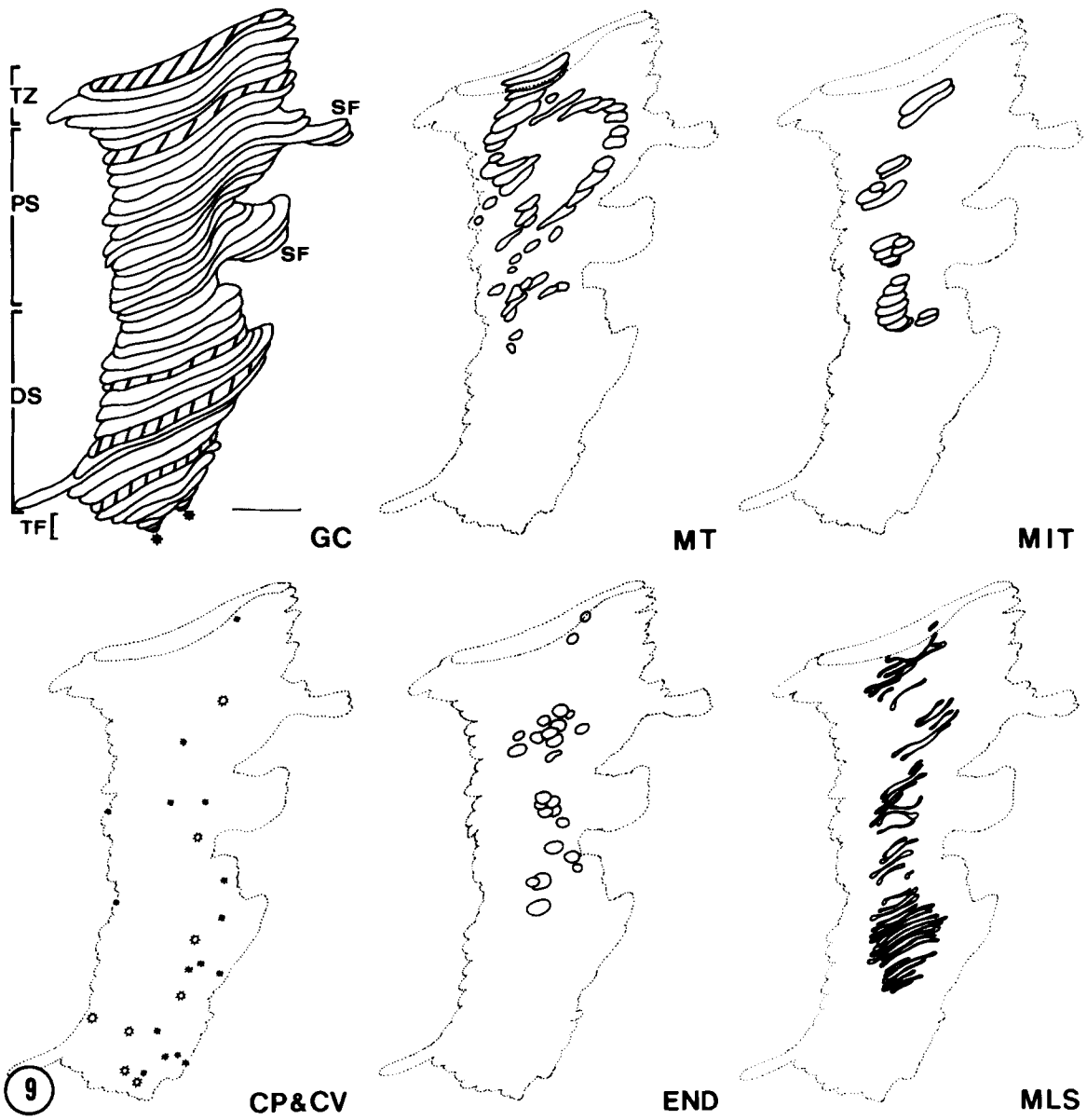

FIGURE 9 Spatial distributions of intracellular organelles in a reconstructed growth cone. The images were regraphed manually from the original computer-aided reconstructions of the growth cone, such as the one shown in Fig. 4. Sections 6, 25, 90, 102, and 116 from Fig. 8 are indicated by shading. These line drawings depict the three-dimensional structure of the growth cone (*GC*) and the distribution of its cytoplasmic components: microtubles, *MT*; mitochondria, *MIT*; coated pits, *CP*; coated vesicles, *CV*; endosomes, *END*; multilamellated stacks of lumenless membrane-bound profiles, *MLS*. The structural domains of the growth cone are (a) transition zone (*TZ*, 15 sections or 1.35 μm long); (*b*) proximal segment (*PS*, 54 sections or 4.86 μm long); (*c*) distal segment (*DS*, 54 sections or 4.86 μm long); and (*d*) terminal filopodium (*TF*, 88 sections or 7.92 μm long). The actual length of the terminal filopodium, which branches into two microspikes (*), is not visible at this orientation. Each area indicated for microtubules represents from 5 to 25 microtubules. Areas indicated for mitochondria represent sections of one mitochondrium, so there are seven mitochondria in this growth cone. Areas drawn in figures labeled CP & CV, END, and MLS represent individual membrane-bound organelles, so there are 17 CPs and 8 CVs in this growth cone. *SF*, subterminal filopodium. Bar, 1 μm.

between primary growth cones growing in the brain and regenerating growth cones growing in a culture dish.

Polarized Compartmentalization of Cytoplasmic Organelles in Growth Cones

Except for multilamellated stacks of lumenless membrane-bound profiles, the intracellular organelles in quick-frozen growth cones observed after freeze substitution are comparable to those observed with conventional methods (8, 10, 23, 27, 32, 37). However, a specific distribution of each type of organelle is revealed by the present serial reconstructions of 10 growth cones from the developing optic tectum.

The major organelles in the frozen growth cones are microtubules, mitochondria, endosome-like vesicles and vacuoles, lumenless membrane sacs typically in multilamellated stacks, and coated pits and vesicles. Analysis of their distributions indicates that each type of membrane-bound organelle is concentrated in a particular domain of the growth cone. The spatial polarity of these cytoplasmic organelles, in turn, leads to subdivision the growth cone into distinct structural domains.

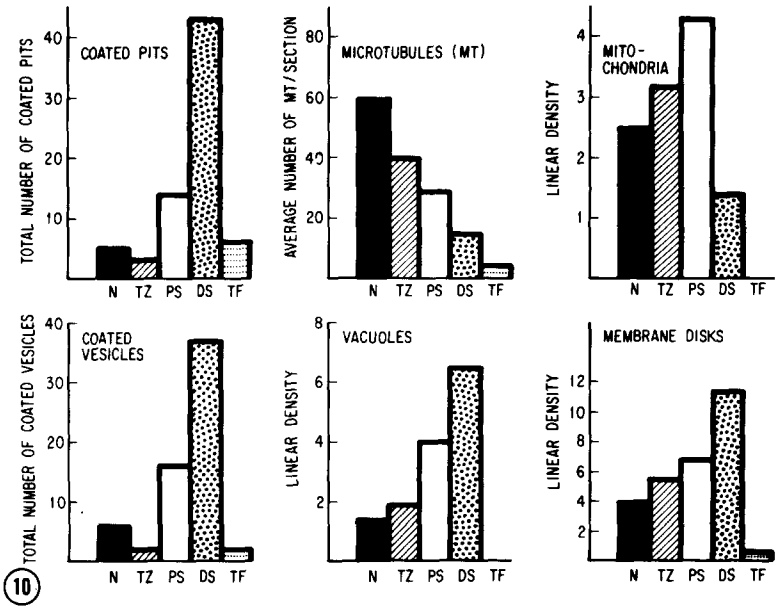

FIGURE 10 Average distribution of various organelles in ten reconstructed growth cones. Characteristics of the five domains of a growth cone, neurite (*N*), transition zone (*TZ*), proximal segment (*PS*) and distal segment (*DS*) of a varicosity, and terminal filopodium (*TF*), are described in the text. Linear density is defined by the number of each type of organelles profile per growth cone section.

Microtubule bundles, which are prominent in neuritic processes, become less distinct in the transition zone and are essentially absent from the varicosity and the more distal segments of the growth cones. In this respect, the microtubule organization in the growth cones from the chick optic tectum is similar to that reported on the basis of immunofluorescent labeling of cultured growth cones (15a) but differs from the hairpin looping of microtubule bundles in the growth cones of cultured nerve cells (40). This discrepancy may reflect differences in the response of the growth cones to the three-dimensional extracellular matrices they encounter in vivo, in contrast to their planar substrate in vitro, as well as differences in developmental stages in microtubule organization (40). It is not clear why the fascicular organization of microtubules becomes progressively and systematically disorganized. However, the less organized microtubule fascicles might facilitate distribution and unloading of anterogradely transported materials in the proximal segment of growth cones if the organized microtubules fascicles serve as channels for axonal transport (30).

The cytoplasm of the most distal domain of a growth cone, the terminal filopodium, consists of a fibrillar meshwork. This fibrillar meshwork is also present in the subplasmalemmal cortical region of the varicosity as well as in the subterminal filopodia, but it is concentrated in the terminal filopodium. The nature of this filamentous material is not clear, but actin and other cytoskeleton-related proteins (myosin, alpha-actinin, gelsolin, and others) are major components (19, 21, 36, 43). Based on the actinomyosin contraction model in non-muscle cells (13, 19, 39), and the known regulatory function of gelsolin on actin gel-sol transformation (42), it is conceivable that this organelle-poor fibrillar meshwork is responsible for most, if not all, motile behavior of the terminal filopodium (40a, 41).

Coated pits and coated vesicles are markedly concentrated within the distal segment of the growth cones. They are seen most frequently near the beginning of the terminal filopodium, less frequently at the initiation of the subterminal filopodia, and rarely in the more proximal region of the growth cone, suggesting that plasmalemmal domains specific for coated-pit formation may be located preferentially, though not exclusively, near the terminal filopodium, where the nonlattice form of clathrin (6, 7) may be also localized. In the neuromuscular junction, endocytosis by coated pits is spatially separated from the exocytotic region at the active zone (14, 22) and high concentrations of cytosolic clathrin are also localized in the presynaptic terminals (7). Thus, the organelles in the growth cone responsible for membrane internalization, the coated pits and coated vesicles, appear to be partially separated from other more proximal membrane-bound organelles (lumenless membrane-bound sacs and the multilamellated stacks).

It is clear from the anatomical organization that the coated pits and the coated vesicles, the endosome-like vesicles and vacuoles, the multilamellated stacks, and the lumenless membrane-bound sacs, are differentially distributed in a manner that suggests a succession of functional states. The spatial differentiation of the distal segment of the growth cone, like that in the terminals of the neuromuscular junction (14, 23), may be related to recycling of its plasmalemma during elongation; this idea is being investigated.

We thank Mr. John Murphy for his excellent photographic work, and Mr. Dave Claypool and Carl Zeiss, Inc., from whom we borrowed the Videoplan Graphic System.

Received for publication 2 April 1985, and in revised form 4 June 1985.

REFERENCES

1. Bentley, D., and H. Keshishian. 1982. Pathfinding by peripheral pioneer neurons in grasshoppers. *Science (Wash. DC).* 218:1082–1088.
2. Bray, D., C. Thomas, and G. Shaw. 1978. Growth cone formation in cultures of sensory neurons. *Proc. Natl. Acad. Sci. USA.* 75:5226–5229.
3. Bridgman, P. C., and T. S. Reese. 1984. The structure of cytoplasm in directly frozen cultured cells. I. Filamentous meshworks and the cytoplasmic ground substances. *J. Cell Biol.* 99:1655–1668.
4. Bunge, M. B. 1973. Fine structure of nerve fibers and growth cones of isolated sympathetic neurons in culture. *J. Cell Biol.* 56:713–735.
5. Bunge, M. B. 1977. Initial endocytosis of peroxidase or ferritin by growth cones of cultured nerve cells. *J. Neurocytol.* 6:407–439.
6. Cheng, T. P. O., and G. J. Wood. 1982. Compartmentalization of clathrin at synaptic terminals. *Brain Res.* 239:201–212.
7. Cheng, T. P. O., F. I. Byrd, J. N. Whitaker, and G. J. Wood. 1980. Immunocytochemical localization of coated vesicle protein in rodent nervous system. *J. Cell Biol.* 86:624–633.
8. Del-Cerro, M. P., and R. S. Snider. 1968. Studies on the developing cerebellum ultrastructure of growth cones. *J. Comp. Neurol.* 133:341–361.

9. Delong, G. R., and A. J. Coulombre. 1967. The specificity of retinotectal connections studied by retinal grafts onto the optic tectum in chick embryos. *Dev. Biol.* 16:513–531.
10. Fox, G. Q., G. D. Pappas, and D. F. Purpura. 1974. Fine structure of growth cones in medullary Raphe nuclei in the postnatal cat. *Brain Res.* 101:411–425.
11. Hamburger, V., and H. L. Hamilton. 1951. A series of normal stages in the development of the chick embryo. *J. Morphol.* 88:49–92.
12. Harrison, R. G. 1910. The outgrowth of the nerve fiber as a mode of protoplasmic movement. *J. Exp. Zool.* 9:787–846.
13. Hartwig, J. H., and T. P. Stossel. 1975. Isolation and properties of actin, myosin and a new actin-binding protein in rabbit alveolar macrophages. *J. Biol. Chem.* 250:5696–5705.
14. Heuser, J. E., and T. S. Reese. 1973. Evidence for recycling of synaptic vesicle membrane during transmitter release at the frog neuromuscular junction. *J. Cell Biol.* 57:315–344.
15. Heuser, J. E., T. S. Reese, M. J. Dennis, Y. Jan, L. Jan, and L. Evans. 1979. Synaptic vesicle exocytosis captures by quick freezing and correlated with quantal transmitter release. *J. Cell Biol.* 81:275–300.
15a. Jockusch, H., and B. M. Jockusch. 1981. Structural proteins in the growth cone of cultured spinal cord neurons. *Exp. Cell Res.* 131:345–352.
16. Kawana, E., C. Sandri, and K. Akert. 1971. Ultrastructure of growth cones in the cerebellar cortex of the neonatal rat and cat. *Z. Zellforsch. Mikrosk. Anat.* 115:284–298.
17. Lance-Jones, C., and L. Landmesser. 1981. Pathway selection by chick lumbrosacral motoneurons during normal development. *Proc. R. Soc. Lond. B. Biol. Sci.* 214:1–18.
18. Landis, S. C. 1978. Growth cone of cultured sympathetic neurons contain adrenergic vesicles. *J. Cell Biol.* 78:R8–R14.
19. Letourneau, P. C. 1981. Immunocytochemical evidence for co-localization in neurite and growth cones of actin and myosin and their relationships to cell-substratum adhesions. *Dev. Biol.* 85:113–122.
20. Letourneau, P. C. 1983. Axonal growth and guidance. *Trends Neurosci.* 6:451–455.
21. Marchisio, P. C., M. Osborn, and K. Weber. 1978. Changes in intracellular organization of tubulin and actin in N-18 neuroblastoma cells during the process of axon extension induced by serum deprivation. *Brain Res.* 155:229–237.
22. Miller, T. M., and J. E. Heuser. 1984. Endocytosis of synaptic vesicle membrane at the frog neuromuscular junction. *J. Cell Biol.* 98:685–698.
23. Nordlander, R. H., and M. Singer. 1982. Morphology and position of growth cones in the developing *Xenopus* spinal cord. *Dev. Brain Res.* 4:181–193.
24. Pfenninger, K. H. 1979. Subplasmalemmal vesicle clusters: real or artifact? *In* Freeze Fracture; Method, Artifacts and Interpretation. J. E. Rash and C. S. Hudson, editors. Raven Press, NY. 71–80.
25. Pfenninger, K. H., and R. P. Bunge. 1974. Freeze-fracturing of nerve growth cones and young nerve fibers. A study of developing plasma membrane. *J. Cell Biol.* 63:180–196.
26. Pfenninger, K. H., and M. Maylie-Pfenninger. 1981. Lectin labeling of sprouting neurons. I. Regional distribution of surface glycogonjugates. *J. Cell Biol.* 89:536–546.
27. Povlishoch, J. T. 1976. The fine structure of the axons and growth cones of the human fetal cerebral cortex. *Brain Res.* 114:379–389.
27a. Rager, G. H. 1980. Development of the retinotectal projection in the chicken. *Adv. Anat. Embryol. Cell Biol.* 63:1–90.
28. Raper, J. A., M. J. Bastiani, and C. S. Good. 1983. Pathfinding by neuronal growth cones in grasshopper embryos. I. Divergent choices made by the growth cones of sibling neurons. *J. Neurosci.* 3:20–30.
29. Rees, R. P., and T. S. Reese. 1981. New structural feature of freeze-substituted neutritic growth cones. *Neuroscience.* 6:247–254.
30. Schnapp, B. J., and T. S. Reese. 1982. Cytoplasmic structure in rapid-frozen axons. *J. Cell Biol.* 94:667–679.
31. Seiki, K., D. Sandquist, L. Williams, and T. H. Williams. 1980. Growth cones in differentiated neuroblastoma: a time-lapse cinematographic and electron microscopic study. *J. Neurocytol.* 9:591–602.
32. Skoff, R. P., and V. Hamburger. 1974. Fine structure of dendritic and axonal growth cones in embryonic chick spinal cord. *J. Comp. Neurol.* 153:107–148.
33. Small, R. K., and K. H. Pfenninger. 1984. Components of the plasma membrane of growing axons. I. Size and distribution of intramembrane particles. *J. Cell Biol.* 98:1422–1433.
34. Solomon, F. 1981. Guiding growth cones. *Cell.* 24:279–280.
35. Speidel, C. C. 1933. Studies of living nerve. II. Activities of ameboid growth cones, sheath cells and myelin segments as revealed by prolonged observation of individual nerve fibers in frog tadpoles. *Am. J. Anat.* 52:1–75.
36. Spooner, B. S., and C. R. Holladay. 1981. Distribution of tubulin and actin in neurites and growth cones of differentiating nerve cells. *Cell. Motil.* 1:167–178.
37. Tennyson, V. M. 1970. The fine structure of the axon and growth cone of the dorsal root neuroblast of the rabbit embryo. *J. Cell Biol.* 44:62–79.
38. Thanos, S., and F. Bonhoeffer. 1983. Investigations on the development and tographic order of retinotectal axons: anterograde and retrograde staining of axons and perikarya with rhodamine in vivo. *J. Comp. Neurol.* 219:420–430.
39. Trinick, J., and G. Offer. 1979. Cross-linking of actin filaments by heavy meromyosin. *J. Mol. Biol.* 133:549–556.
40. Tsui, H. T., K. L. Lanford, H. Ris, and W. L. Klein. 1984. Novel organization of microtubules in culture central nervous system neurons: formation of hair-pin loops at ends of maturing neurites. *J. Neurosci.* 4:3002–3013.
40a. Wessels, N. K., B. S. Spooner, J. F. Ash, M. O. Bradley, M. Luduena, E. Taylor, J. T. Wrenn, and K. M. Yamada. 1971. Microfilaments in cellular and developmental processes. *Science (Wash. DC).* 171:135.
41. Yamada, K. M., B. S. Spooner, and N. K. Wessels. 1971. Ultrastructural and function of growth cones and axons of cultured nerve cells. *J. Cell Biol.* 49:614–635.
42. Yin, H. L., and T. P. Stossel. 1979. Control of cytoplasmic actin gel-sol transformation by gelsolin, a calcium dependent regulatory protein. *Nature (Lond.).* 281:583–586.
43. Yin, H. L., J. H. Albrecht, and A. Fattoum. 1981. Identification of gelsolin, a Ca^{+2}-dependent regulatory protein of actin gel-sol transformation, and its intracellular distribution in a variety of cells and tissues. *J. Cell Biol.* 91:901–906.